Interference patterns of superfluid Fermi gases in the BCS-BEC crossover released from optical lattices

Wen Wen and Yu Zhou
Department of Physics and Institute of Theoretical Physics, East China Normal University, Shanghai 200062, China

Guoxiang Huang*
State Key Laboratory of Precision Spectroscopy and Department of Physics, East China Normal University, Shanghai 200062, China
(Received 22 October 2007; published 21 March 2008)

We study the interference patterns of a superfluid Fermi gas released from optical lattices below and above Feshbach resonance based on a simple phenomenological approach. We first solve the order-parameter equation valid for the crossover from Bardeen-Cooper-Schrieffer (BCS) superfluid to a Bose-Einstein condensate (BEC) to obtain an initial distribution of subcondensates formed in an optical lattice. Then we investigate the coherent evolution of the subcondensates when both harmonic oscillator and optical lattice potentials are switched off. The interference patterns of the superfluid Fermi gas along the BCS-BEC crossover during a nearly ballistic expansion are calculated by means of Feynman propagator method combined with numerical simulations. The result obtained agrees with the recent experimental observation reported by the MIT group [J. K. Chin *et al.*, Nature (London) **443**, 961 (2006)].

DOI: 10.1103/PhysRevA.77.033623 PACS number(s): 03.75.Ss, 03.75.Lm

I. INTRODUCTION

The problem of BCS-BEC crossover, which is not only of fundamental interest in condensed matter physics but also closely related to the understanding of the physical mechanism of high-T_c superconductivity, has attracted considerable attention for decades [1–3]. Recent studies showed that such a problem can be investigated by using ultracold fermionic atomic gases through a magnetic field induced Feshbach resonance, by which the magnitude and sign of interatomic interactions can be tuned in a controllable way [4,5].

Optical lattices are regular arrays of potential wells created by one or more sets of orthogonal intersecting laser beams, which provide a periodic potential for ultracold atoms [2–6]. In the case of Fermi gases the study is closely related to the physics of electrons in metals and semiconductors, and hence Fermi gases in optical lattices can be used to make detailed quantum simulations of the many-body physics of solid-state materials. Due to the advantages of easy manipulation on optical lattice potentials and specific characters of ultracold atom gases, such quantum simulations may provide many useful insights for strongly correlated condensed matter systems [2–6].

An important topic in the study of ultracold Fermi gases in optical lattices is a direct observation of superfluid property in the BCS-BEC crossover. One expects that interference patterns appear when subcondensates formed by condensed fermionic atom pairs in an optical lattice expand ballistically and overlap each other. Such behavior has been observed successfully in a recent experiment carried out by Chin *et al.* [7] for a superfluid ^{6}Li Fermi gas. The measurement in Ref. [7] was made on both sides of a Feshbach resonance by using a magnetic field ramp that increased rapidly the detuning from the Feshbach resonance, and hence took the system out of the strongly interacting regime and enforced a nearly ballistic expansion of the gas. By this useful fast magnetic field ramp technique, clear interference patterns of condensate wave function after the nearly ballistic expansion have been obtained, which provided a very clear evidence for the superfluidity of ultracold fermions in optical lattices.

A complete understanding of the long-range phase coherence behavior reported in Ref. [7] is not an easy problem. In principle, one can start from a model Hamiltonian that includes the main character of the ultracold Fermi gas in the optical lattice in the BCS-BEC crossover. Because the fermionic atom pairs are trapped in combined harmonic oscillator and optical lattice potentials, the inhomogeneous and mesoscopic features of the system make a microscopic approach of the problem difficult. However, notice that for a shallower optical lattice depth the system is in a superfluid regime and hence at ultralow temperature the condensed fermionic atom pairs do not decay into single atoms due to the existence of energy gap in their excitation spectrum. It is known the dynamics of such perfect superfluid can be well described phenomenologically by using an order-parameter equation, i.e., a generalized nonlinear Schrödinger (GNLS) equation, obtained by time-dependent density functional theory [8–17]. Different superfluid regimes can be characterized by an equation of state, which can be obtained by a quantum Monte Carlo simulation [18,19]. The GNLS equation captures a dominant feature that the superfluid exhibits macroscopically, though its mathematical framework is simple. Recently, the GNLS equation has been used to investigate the collective excitations and ballistic expansions of superfluid Fermi gases, and the results obtained agree quite well with experimental ones [9–14,17].

In this work, we extend the work of Refs. [9–17] to study the formation of interference patterns of a superfluid Fermi gas released from an optical lattice by using a simple phenomenological approach. The interference patterns of the su-

*Corresponding author: gxhuang@phy.ecnu.edu.cn

 ©2008 The American Physical Society

perfluid Fermi gas along the BCS-BEC crossover during a nearly ballistic expansion will be investigated by an approximate analytical treatment combined with numerical simulations. The method is simple and the result for interference patterns obtained in different superfluid regimes agrees fairly well with the experimental one.

The paper is arranged as follows. Section II gives a simple introduction of the GNLS equation used to describe the superfluid dynamics of fermionic pair condensates. Section III provides the initial distribution of fermionic pair subcondensates formed in a three-dimensional (3D) optical lattice through solving the GNLS equation. The coherent evolution of the subcondensates after switching off combined harmonic and optical lattice potentials is investigated by means of the Feynman propagator method and interference patterns of the superfluid Fermi gas are calculated by using a numerical simulation. The result obtained is compared with the experimental one reported in Ref. [7]. The last section contains discussion and summary of our main results.

II. ORDER-PARAMETER EQUATION ALONG THE BCS-BEC CROSSOVER

We consider a system of superfluid Fermi (i.e., ^{6}Li or ^{40}K) gas in which fermionic atoms have two different internal states and atomic numbers in each internal state are the same. In ground state condensed fermionic atom pair density is $n/2$, where n is atomic density. By means of Feshbach resonance the transition from BCS to BEC regimes can be realized through tuning an applied magnetic field and hence changing the s-wave scattering length a_s. When $a_s<0$ ($a_s>0$), the system is in a BCS (BEC) regime. By defining a dimensionless interaction parameter $\eta \equiv 1/(k_F a_s)$, where $k_F=(3\pi^2 n)^{1/3}$ is Fermi wave number, one can distinguish several different superfluidity regimes [10,13,17], i.e., BCS regime ($\eta<-1$), BEC regime ($\eta>1$), and BEC-BCS crossover regime ($-1<\eta<1$). $\eta=-\infty$ ($\eta=+\infty$) is called BCS (BEC) limit and $\eta=0$ is called unitarity limit. Both theoretical and experimental studies show that the transition from BCS regime to BEC regime is smooth [1–3], which hints that one can study the physical property of the system in various superfluid regimes in a unified way.

At zero temperature, the macroscopic dynamics of the superfluid is governed by the hydrodynamic equations obtained from a time-dependent density functional theory [9–17]

$$\frac{\partial n}{\partial t}+\nabla\cdot(n\mathbf{v})=0, \tag{1a}$$

$$m\frac{\partial \mathbf{v}}{\partial t}+\nabla\left[\frac{1}{2}m\mathbf{v}^2+\mu(n)+V^{\mathrm{ho}}(\mathbf{r})\right]=0, \tag{1b}$$

where $\mathbf{v}$ is superfluid velocity, m is atomic mass, and $V^{\mathrm{ho}}(\mathbf{r})$ is a harmonic trapping potential. The equation of state (also called bulk chemical potential) under a local density approximation has the form $\mu(n)=\partial[n\varepsilon(n)]/\partial n$, where $\varepsilon(n)$ is the bulk energy per particle obtained by taking $V^{\mathrm{ho}}(\mathbf{r})=0$ [20]. Introducing $\varepsilon(n)=(3/5)\varepsilon_F\sigma(\eta)$, with $\varepsilon_F=\hbar^2k_F^2/(2m)$ being Fermi energy, one obtains [10–17]

$$\mu(n)=\varepsilon_F\left(\sigma(\eta)-\frac{\eta}{5}\frac{\partial\sigma(\eta)}{\partial\eta}\right). \tag{2}$$

As a function of n, the expression of $\mu(n)$ is very complicated, which prevents us from obtaining analytical results on the dynamics of the system. A simple approach is to take a polytropic approximation, i.e., by assuming [9–17,21–23] $\mu(n)=\mu^0(n/n^0)^\gamma$ with

$$\gamma=\gamma(\eta^0)=\left(\frac{n}{\mu}\frac{\partial\mu}{\partial n}\right)_{\eta=\eta^0}=\frac{\frac{2}{3}\sigma(\eta^0)-\frac{2\eta^0}{5}\sigma'(\eta^0)+\frac{(\eta^0)^2}{15}\sigma''(\eta^0)}{\sigma(\eta^0)-\frac{\eta^0}{5}\sigma'(\eta^0)}, \tag{3}$$

where μ^0 and n^0 are respectively reference chemical potential and particle number density of the system, introduced here for the convenience of later calculation. In the following, we take n^0 to be the equilibrium superfluid density at the center of the trapping potential. Thus one has $\mu^0=\varepsilon_F^0[\sigma(\eta^0)-\eta^0\sigma'(\eta^0)/5]$, with $\varepsilon_F^0=(\hbar k_F^0)^2/(2m)$, $\eta^0=1/(k_F^0a_s)$, and $k_F^0=(3\pi n^0)^{1/3}$. There are two well known limits for the value of the polytropic index γ. One is $\gamma=2/3$ at $\eta^0\to-\infty$ (BCS limit) and another one is $\gamma=1$ at $\eta^0\to+\infty$ (BEC limit). The polytropic approximation has the advantage of allowing one to obtain analytical results for various superfluid regimes in a unified way. In fact, it is quite accurate because γ is a slowly varying function of η^0 and hence widely used in literature [9–17,21–23].

For studying the interference patterns when the condensate is released from the optical lattice, we need a wave equation for the superfluid order parameter, which can be obtained in the following way. Notice that at $T=0$ the system consists of only condensed fermionic atom pairs. The order parameter of the condensate can be expressed as $\langle\hat{\psi}_a(\mathbf{r}-\boldsymbol{\rho}/2)\hat{\psi}_b(\mathbf{r}+\boldsymbol{\rho}/2)\rangle$, where $\hat{\psi}_j(\mathbf{r}\pm\boldsymbol{\rho}/2)$ is the Fermi annihilation operator that destroys one fermion in the internal state j ($j=a$ or b; $a\neq b$) and at location $\mathbf{r}\pm\boldsymbol{\rho}/2$. For a superfluid with velocity $\mathbf{v}_s$, the momentum of each particle is boosted by an amount $m\mathbf{v}_s$ and the order parameter $\langle\hat{\psi}_a(\mathbf{r}-\boldsymbol{\rho}/2)\hat{\psi}_b(\mathbf{r}+\boldsymbol{\rho}/2)\rangle$ will be multiplied by a factor $\exp(2i\phi)$ with $\phi=m\mathbf{v}_s\cdot\mathbf{r}/\hbar$. Obviously, $\Phi_s\equiv 2\phi=M\mathbf{v}_s\cdot\mathbf{r}/\hbar$ is the phase of $\langle\hat{\psi}_a(\mathbf{r}-\boldsymbol{\rho}/2)\hat{\psi}_b(\mathbf{r}+\boldsymbol{\rho}/2)\rangle$ and one has $\mathbf{v}_s=(\hbar/M)\nabla\Phi_s$. The change in the phase of the order parameter is independent of the relative coordinate ρ and thus we can put ρ to zero [4].

Note that $n_s=n/2$ and $\mathbf{v}\approx\mathbf{v}_s$ (valid in continuity approximation), where n and $\mathbf{v}$ are the quantities given in Eqs. (1a) and (1b). Using these relations, Eqs. (1a) and (1b) can be transferred into the following form:

$$\frac{\partial n_s}{\partial t}+\nabla\cdot(n_s\mathbf{v}_s)=0, \tag{4a}$$

$$M\frac{\partial \mathbf{v}_s}{\partial t}+\nabla\left[\frac{1}{2}M\mathbf{v}_s^2+\mu_s(n_s)+V_s^{\mathrm{ho}}(\mathbf{r})\right]=0, \tag{4b}$$

with $\mu_s(n_s)=2\mu(2n_s)$ and $V_s^{\mathrm{ho}}(\mathbf{r})=2V^{\mathrm{ho}}(\mathbf{r})$. If a quantum pressure term $-\hbar^2\nabla^2\sqrt{n_s}/(2M\sqrt{n_s})$ is included, which was done in Ref. [9], and later on in Refs. [10–17], the hydrodynamic

Eqs. (4a) and (4b) can be simplified to the GNLS equation

$$i\hbar\frac{\partial\Psi_s}{\partial t}=\left[-\frac{\hbar^2\nabla^2}{2M}+V_s^{\mathrm{ho}}(\mathbf{r})+\mu_s(n_s)\right]\Psi_s, \tag{5}$$

where we have introduced $\Psi_s(\mathbf{r},t)=\sqrt{n_s}\exp(i\Phi_s)$, which is the order parameter of the condensed fermionic atomic pairs. It is easy to show that in the BEC limit (i.e., $\gamma=1$) the GNLS Eq. (5) coincides exactly with the order-parameter equation derived in Ref. [24] based on Bogoliubov–de Gennes equations in an extended BCS theory.

III. INTERFERENCE PATTERNS

A. Time evolution of the condensate wave function

Now we begin to the investigate the interference pattern of the Fermi gas in the superfluid regime based on the order parameter Eq. (5). We assume that the condensate is prepared in a harmonic oscillator potential

$$V_s^{\mathrm{ho}}(\mathbf{r})=M[\omega_x^2x^2+\omega_y^2y^2+\omega_z^2z^2]/2, \tag{6}$$

where ω_j $(j=x,y,z)$ is the trapping frequency in the jth direction. Then a three-dimensional (3D) optical lattice potential

$$V_s^{\mathrm{op}}(\mathbf{r})=sE_R[\sin^2(qx)+\sin^2(qy)+\sin^2(qz)], \tag{7}$$

formed by three orthogonal intersecting laser beams, is added to the system. Here the wave vector $q=2\pi/\lambda$ is fixed by the laser wavelength λ. The period of the optical lattice is $d=\lambda/2$, which is much smaller than the size of the condensate. The lattice potential depth sE_R is measured in units of the recoil energy $E_R=\hbar^2q^2/(2M)$ with s being a dimensionless parameter determining the intensity of the laser field.

Due to the introduction of the optical lattice, in equilibrium the system is composed of many subcondensates located in minima of the combined potential $V_s(\mathbf{r})=V_s^{\mathrm{ho}}(\mathbf{r})+V_s^{\mathrm{op}}(\mathbf{r})$. Since we are interested in the interference pattern of the superfluid Fermi gas during a free expansion, the initial distribution of the condensate wave function $\Psi_s(\mathbf{r},0)$ must be calculated before the combined potential is switched off.

Notice that at present a rigorous analytical result for this initial distribution is not yet available. Here we employ the technique developed in Refs. [25,26] to obtain an approximate expression for equilibrium subcondensates of the system. Since the size of the whole condensate is much larger than that of each subcondensate, if optical lattice depth is moderately big the optical lattice potential can be expressed by a superposition of many approximate harmonic potentials, i.e.,

$$V_s^{\mathrm{op}}(\mathbf{r})=\frac{M\omega_{\mathrm{op}}^2}{2}\left[\sum_{k_x}(x-k_xd)^2+\sum_{k_y}(y-k_yd)^2+\sum_{k_z}(y-k_zd)^2\right], \tag{8}$$

where the effective trapping frequency is defined by $\omega_{\mathrm{op}}=2\sqrt{s}E_R/\hbar$, which is much larger than the frequencies ω_j of the harmonic oscillator potential. We assume that typical width of subcondensates is much less than the optical lattice period d and consider the case that the subcondensates in different lattice sites are fully coherent (i.e., the whole system is in a superfluid state). In this situation the chemical potentials of these subcondensates are identical and hence under a tight-binding approximation [25,26] the condensate wave function of the system can be written as the form

$$\Psi_s(\mathbf{r},t)=\sum_{k_x,k_y,k_z}\psi_{k_x,k_y,k_z}(\mathbf{r})\exp(-i\mu_Gt/\hbar), \tag{9}$$

where μ_G is the chemical potential of the system and (k_x,k_y,k_z) denote the central positions of various subcondensates.

Substituting Eq. (9) into Eq. (5) we obtain the equation for ψ_{k_x,k_y,k_z}

$$\left\{-\frac{\hbar^2\nabla^2}{2M}+\frac{1}{2}M[\omega_x^2x^2+\omega_y^2y^2+\omega_z^2z^2]+\frac{1}{2}M\omega_{\mathrm{op}}^2[(x-k_xd)^2+(y-k_yd)^2+(z-k_zd)^2]+\mu_s^0\left(\frac{n_s}{n_s^0}\right)^\gamma\right\}\psi_{k_x,k_y,k_z}=\mu_G\psi_{k_x,k_y,k_z}, \tag{10}$$

where $\mu_s^0=\mu_s(n_s^0)$. In obtaining Eq. (10) the small overlap of the subcondensates between adjacent sites has been ignored. After the transformation $x-k_xd\to x$, $y-k_yd\to y$, and $z-k_zd\to z$, Eq. (10) becomes

$$\left[-\frac{\hbar^2\nabla^2}{2M}+\frac{1}{2}M[\omega_x^2(x+k_xd)^2+\omega_y^2(y+k_yd)^2+\omega_z^2(z+k_zd)^2]+\frac{1}{2}M\omega_{\mathrm{op}}^2(x^2+y^2+z^2)+\mu_s^0\left(\frac{n_s}{n_s^0}\right)^\gamma\right]\psi_{k_x,k_y,k_z}=\mu_G\psi_{k_x,k_y,k_z}. \tag{11}$$

Because $\omega_{\mathrm{op}}\gg\omega_j$ $(j=x,y,z)$, for the subcondensate confined in the lattice site (k_x,k_y,k_z) it is evident that one has $x\ll k_xd$, $y\ll k_yd$, and $z\ll k_zd$. Thus Eq. (11) can be simplified into

$$\left[-\frac{\hbar^2\nabla^2}{2M}+\frac{1}{2}M\omega_{\mathrm{op}}^2(x^2+y^2+z^2)+\mu_s^0\left(\frac{n_s}{n_s^0}\right)^\gamma\right]\psi_{k_x,k_y,k_z}=\mu_{k_x,k_y,k_z}\psi_{k_x,k_y,k_z}, \tag{12}$$

where we have introduced the notation $\mu_{k_x,k_y,k_z}=\mu_G-(M/2)d^2(\omega_x^2k_x^2+\omega_y^2k_y^2+\omega_z^2k_z^2)$. Equation (12) describes a subcondensate trapped in a harmonic oscillator potential with an isotropic trapping frequency ω_{op}. The subcondensate has an effective chemical potential μ_{k_x,k_y,k_z} and its central position is at the site (k_x,k_y,k_z).

The particle-number distribution N_{k_x,k_y,k_z} in each subcondensate can be obtained by solving Eq. (12) under a Thomas-Fermi approximation. We obtain

$$N_{k_x,k_y,k_z} = N_0\left(1 - \frac{\omega_x^2 k_x^2}{\omega_{\rm ho}^2 k_M^2} - \frac{\omega_y^2 k_y^2}{\omega_{\rm ho}^2 k_M^2} - \frac{\omega_z^2 k_z^2}{\omega_{\rm ho}^2 k_M^2}\right)^{2+3\gamma/2\gamma}, \tag{13}$$

where $N_0=(2\pi/M\omega_{\rm op}^2)^{3/2}(Md^2\omega_{\rm ho}^2 k_M^2/2)^{3/2+1/\gamma}n_s^0\Gamma(1/\gamma+1)/[(\mu_s^0)^{1/\gamma}\Gamma(1/\gamma+5/2)]$ is the particle number at central site (0, 0, 0), $\omega_{\rm ho}=(\omega_x\omega_y\omega_z)^{1/3}$ is mean trapping frequency of the harmonic oscillator potential (6), and Γ is the gamma function. The chemical potential of the system is expressed as $\mu_G \equiv Md^2\omega_{\rm ho}^2 k_M^2/2$, with

$$k_M = \left[\frac{N}{n_s^0}\frac{\Gamma(4+1/\gamma)}{\Gamma(1+1/\gamma)}\left(\frac{2\mu_s^0}{M}\right)^{1/\gamma}\frac{\omega_{\rm op}^3}{\pi^3(\omega_{\rm ho}d)^{2+3\gamma/\gamma}}\right]^{\gamma/6\gamma+2}. \tag{14}$$

By Eq. (13) the possible values of k_j $(j=x,y,z)$ should be limited to the condition

$$\frac{k_x^2}{(\omega_{\rm ho}^2/\omega_x^2)} + \frac{k_y^2}{(\omega_{\rm ho}^2/\omega_y^2)} + \frac{k_z^2}{(\omega_{\rm ho}^2/\omega_z^2)} \le k_M^2. \tag{15}$$

The normalized initial superfluid wave function of the system in both the harmonic oscillator potential (6) and the optical lattice potential (7) can be approximated by a sum of Gaussian wave functions centered at different potential minima

$$\Psi_s(x,y,z,t=0) = A_n{\sum_{\mathbf{k}}}'\left(1 - \frac{\omega_x^2 k_x^2}{\omega_{\rm ho}^2 k_M^2} - \frac{\omega_y^2 k_y^2}{\omega_{\rm ho}^2 k_M^2} - \frac{\omega_z^2 k_z^2}{\omega_{\rm ho}^2 k_M^2}\right)^{2+3\gamma/4\gamma} \times \exp\left[-\frac{(x-k_x d)^2+(y-k_y d)^2+(z-k_z d)^2}{2\xi_{k_x,k_y,k_z}^2}\right], \tag{16}$$

where A_n is a normalized constant, and the prime in the sign of the sum means that the summation is limited to the domain indicated by the inequality (15). We assume that the number of fermionic atom pairs in each lattice site is not large, so the width of the subcondensate ξ_{k_x,k_y,k_z} can be approximately replaced by the harmonic oscillator length $a_{\rm op} \equiv [\hbar/(M\omega_{\rm op})]^{1/2}$. In this situation one has $A_n=\{\Gamma(1/\gamma+4)/[\Gamma(1/\gamma+5/2)(k_M\pi a_{\rm op})^3]\}^{1/2}$.

The time evolution of the superfluid Fermi gas after releasing from the harmonic oscillator potential (6) and optical lattice potential (7) can be obtained through solving the GNLS Eq. (5) by taking Eq. (16) as an initial condition. Generally, the interaction among atoms may induce elastic collisions during an expansion and hence change the momentum distribution and remove a significant fraction of atoms from the subcondensates. As a result, the interference peaks of the condensate wave function will be washed out. However, in the experiment of Chin *et al.*, a nearly ballistic expansion of the superfluid Fermi gas is obtained by applying a fast magnetic field ramp technique [7]. Thus in a leading order approximation one can employ the famous Feynman propagator method [27] to obtain the condensate wave function for any time $t>0$ [26–28]. Then we have

$$\Psi_s(x,y,z,t) = \int_{-\infty}^{\infty}dx'\int_{-\infty}^{\infty}dy'\int_{-\infty}^{\infty}dz' \times G(x,y,z,t;x',y',z',t'=0)\Psi_s(x',y',z',t'=0). \tag{17}$$

The propagator $G(x,y,z,t;x',y',z',t'=0)$ in Eq. (17) is given by

$$G(x,y,z,t;x',y',z',t'=0) = \prod_{j=1}^{3} G_j(x_j,t;x_j',t'=0) \tag{18}$$

with

$$G_j(x_j,t;x_j',t'=0) = \left(\frac{2\pi i\hbar t}{M}\right)^{-1/2}\exp[iM(x_j-x_j')^2/2\hbar t] \tag{19}$$

being the component of the propagator in the jth direction. In Eqs. (18) and (19) we have used the notations $(x_1,x_2,x_3) \equiv (x,y,z)$.

Implementing the integration in Eq. (17) we obtain

$$\Psi_s(x,y,z,t) = A_n{\sum_{k_x,k_y,k_z}}'\left(1 - \frac{\omega_x^2 k_x^2+\omega_y^2 k_y^2+\omega_z^2 k_z^2}{\omega_{\rm ho}^2 k_M^2}\right)^{2+3\gamma/4\gamma} \times \prod_{j=1}^{3}\Omega_j(x_j,t), \tag{20}$$

where

$$\Omega_j(x_j,t) = \left(\frac{1}{1+i\alpha(t)}\right)^{1/2}\exp\left\{-\frac{(x_j-k_j d)^2}{2a_{\rm op}^2[1+i\alpha(t)]}\right\} \tag{21}$$

with $\alpha(t)=\hbar t/(Ma_{\rm op}^2)$. By Eqs. (20) and (21) one can calculate the density distribution of the superfluid Fermi gas $n_s(x,y,z,t)=N|\Psi_s(x,y,z,t)|^2$ numerically, which will be presented in the next subsection.

B. Interference patterns of the superfluid Fermi gas

In the recent MIT experiment by Chin *et al.* [7], high-contrast interference patterns of fermion pair subcondensates released from combined harmonic oscillator and 3D optical lattice potentials below and above the Feshbach resonance have been observed. This experiment provides a clear signature and direct evidence of the long-range phase coherence of the ultracold Fermi gas [3].

The MIT experiment [7] used a balanced mixture of ^{6}Li fermions in the two lowest hyperfine states. By means of evaporative cooling a condensate containing $N=2\times10^5$ fermion pairs is produced in an anisotropic harmonic oscillator potential, with the trapping frequencies $(\omega_x,\omega_y,\omega_z)=2\pi\times(270,340,200)$ Hz. Then a 3D optical lattice potential formed by three orthogonal intersecting laser beams with wavelength $\lambda=1064$ nm was imposed on the condensate. Using their experimental parameters, we obtain the effective trapping frequency [defined by Eq. (8)] $\omega_{\rm op}=2\pi\times65\,727$ Hz, which is much larger than the trapping frequencies ω_j $(j=x,y,z)$ of the harmonic oscillator potential,

TABLE I. Parameters of the superfluid Fermi gas in the BCS-BEC crossover used in numerical simulations.

	(a)	(b)	(c)	(d)	(e)
B (G)	698	822	867	917	1529
$\eta^0=1/(k_F^0 a_s)$	2.00	0.096	−0.224	−0.480	−1.250
γ	1.05	0.71	0.60	0.60	0.61
μ_s^0/ε_F^0	0.076	0.768	1.132	1.334	1.60
$\bar{R}(\mu\mathrm{m})$	7.2	22.8	27.7	30.1	33.0

justifying the validity of the approximation used from Eq. (11) to Eq. (12). The Fermi energy of the trapped particles is given by $E_F=\hbar(6N\omega_x\omega_y\omega_z)^{1/3}$, which determines the value $1/k_F^0=0.17$ μm. The size of the condensate can be estimated by Thomas-Fermi approximation, which gives the condensate radii $R_j=[2\mu_s^0/(M\omega_j^2)]^{1/2}$ $(j=x,y,z)$, with their geometric mean given by $\bar{R}=(R_xR_yR_z)^{1/3}$.

In order to study the superfluid property of the fermion pairs in the BCS-BEC crossover, Chin *et al.* used the Feshbach resonance technique to tune the s-wave scattering length a_s, which is the function of the applied magnetic field B. Near the resonance one has the approximated expression [7]

$$a_s(B) = -1405a_0[1+0.0004(B-834)]\left[1+\frac{300}{B-834}\right], \tag{22}$$

where a_0 is the Bohr radius. For the optical lattice depth $5E_R$ (which belongs to superfluid regime) and at three different magnetic fields (i.e., $B=822$ G, 867 G, and 917 G, which correspond to $a_s=33558a_0$, $-14365a_0$, and $-6699a_0$, respectively), high-contrast interference patterns with six first-order side peaks clearly visible around the zero-momentum central peak have been observed (see Fig. 2 of Ref. [7]).

We must stress that in the previous experimental observation on the interference patterns of Bose gases [29–31], interparticle interaction is weak and hence the expansion of the gases after releasing from optical lattices can be approximated as a ballistic one. However, for the strongly interacting Fermi gas elastic collisions during the expansion can change the momentum distribution and remove a significant fraction of atoms from the subcondensates, and thus blur the interference peaks. In order to avoid the elastic collisions that may result in diffusion and loss of the Fermi atomic cloud, Chin *et al.* [7] applied a magnetic field ramp that can increase quickly the detuning from Feshbach resonance and hence take the system out of the strongly interacting regime. By using this useful technique, Chin *et al.* [7] acquired a nearly ballistic expansion of the superfluid Fermi gas and hence observed clear interference patterns after the gas is released from the optical lattices. Thus we can apply the formulas obtained by the Feynman propagator method in the last section to calculate the interference patterns and make a comparison between our theoretical result and the experimental one reported by Chin *et al.* [7].

Notice that the fast magnetic field ramp technique was pioneered by Bourdel *et al.* for the observation of the transition to superfluid phase of a Fermi gas near Feshbach resonance [32]. Later on, this technique was also successfully used to the observation of fermionic pair condensates [33], quantized vortices [34], the momentum distribution [35], and vortex lattice expansion of the superfluid Fermi gas in the BCS-BEC crossover [36]. Although the Fermi gas expands nearly ballistically due to the use of the fast magnetic field ramp technique, the interaction effect has been included in the calculation of the ground state wave function (16), which is obtained by taking the mean-field interaction of the superfluid fermions into account before the expansion. Because in this work we pay attention mainly to the nearly ballistic expansion and the subsequent interference patterns, the simulation of the fast magnetic field ramp process before the expansion is beyond the scope of this work [37].

Using the experimental parameters in Ref. [7] we can obtain the values of η^0, $\gamma(\eta^0)$, μ_s^0/ε_F^0, and $\bar{R}$ for different magnetic field B, which for clearness have been listed in Table I. According to the classification given in Sec. II, case (a) in Table I belongs to the BEC regime; cases (b), (c), and (d), which correspond to the three cases considered in Fig. 2 of Ref. [7], belong to the crossover regime; while case (e) belongs to the BCS regime.

After suddenly switching off both the harmonic oscillator and the optical lattice potentials, the subcondensates at the lattice sites expand freely; then they overlap and coherently interfere each other to form an interference pattern, which consists of a central peak and smaller, symmetrically spaced lateral peaks moving in opposite directions. A simple analysis similar to that used in Sec. 13.1.1 of Ref. [4] gives the asymptotic formula of the position between the interference peaks

$$X_{\ell_j} = \pm 2\pi\ell_j\frac{\hbar t}{dM} \quad (j=x,y,z;\ \ell_j=0,1,2,\ldots), \tag{23}$$

where t is the free-expansion time and the integer number ℓ_j denotes the ℓ_jth-order lateral peak in the jth direction.

Figure 1 shows the result of the interference pattern when the gas is released from the combined potentials after 6.5 ms. The pattern is obtained by using the parameters of case (b) in Table I. We see that there is one central peak that locates at the center $(x,y,z)=(0,0,0)$ and six first-order lateral peaks carrying high momentum locate symmetrically at positions $(-764d,-764d,0)$, $(-764d,764d,0)$, $(764d,-764d,0)$,

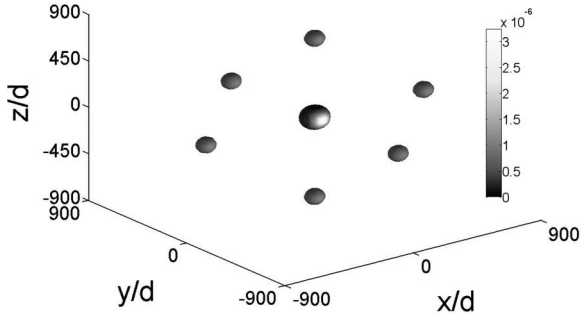

FIG. 1. Interference pattern of the superfluid Fermi gas released from the combined potentials after 6.5 ms ballistic expansion. The pattern is obtained by using the parameters of case (b) in Table I. The value of the condensate density is normalized by N/a_{op}^3.

$(764d,764d,0)$, $(0,0,-764d)$, and $(0,0,764d)$, with $d=532$ nm. After the expansion time 6.5 ms, the first-order lateral peaks (i.e., $\ell_j=1$) locate at $X_{1_j}=\pm 764d=\pm 0.4$ mm with respect to the central peak at $X_{0_j}=0$. The result is a little larger than the experimental value (approximately ± 0.3 mm) reported in Ref. [7]. The reason is that our theoretical approach is based on the assumption that the system is at zero temperature and in a complete superfluid. In addition, the interaction between particles during the expansion, even small in the nearly ballistic expansion, will also have a contribution on the interference pattern.

Experimentally, one usually measures the column number density distribution of the condensed pairs, i.e., $n_{s\perp}(x,y)=\int_{-\infty}^{\infty}dz\ n_s(x,y,z)$. In Fig. 2 we have shown the simulating result of the interference patterns of $n_{s\perp}(x,y)$ in the BCS-BEC crossover when the subcondensates have been released from both the harmonic oscillator and the optical lattice potentials for $t=6.5$ ms. The interference patterns in panels (a), (b), (c), (d), and (e) are obtained by calculating $n_{s\perp}(x,y)$ based on the parameters given in cases (a), (b), (c), (d), and (e) of Table I. In all figures the values of pairs density $n_{s\perp}$ have been normalized by $n_1=N/a_{\mathrm{op}}^2$. We see that from the BEC regime [case (a)], through the crossover regime [cases (b), (c), and (d)], to the BCS regime [case (e)], the interference peaks become wider and their maxima are also lowered gradually. The physical reason for the change of the interference patterns from the BEC regime to the BCS regime can be explained as follows. Because in the BEC (BCS) regime the reference chemical potential μ_s^0 is smaller (larger), the geometric mean radius of the condensate $\bar{R}$ is smaller (larger) (see Table I for detail), which results in a larger (smaller) pair density and hence larger (smaller) peak value and narrower (wider) width of the interference peaks in the BEC (BCS) regime.

In order to show the difference of the interference patterns in different superfluid regimes more clearly, in Fig. 3 we have plotted the number density distribution of condensed pairs $n_{s\perp}(x,y=0)$ in units of N/a_{op}^2. The result is obtained by using the parameters of Table I for cases (a), (c), and (e). We see that there is a larger difference between the interference patterns in different superfluid regimes. The inset shows the

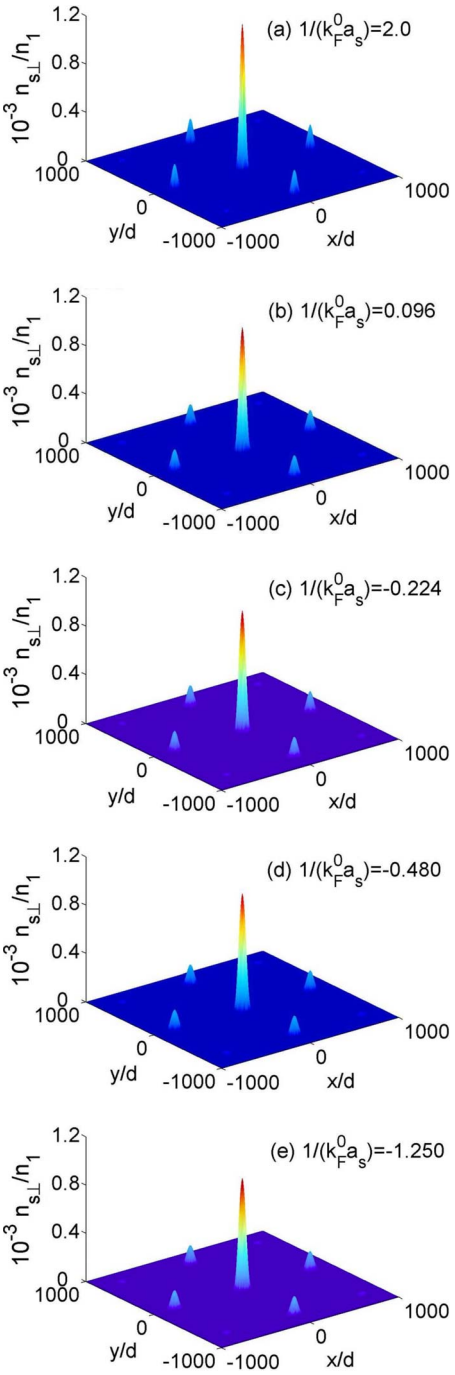

FIG. 2. (Color online) Column pair density distribution $n_{s\perp}(x,y)$ in the BCS-BEC crossover when the subcondensates have been released from both the harmonic oscillator and the optical lattice potentials for $t=6.5$ ms. The interference patterns in panels (a), (b), (c), (d), and (e) are obtained by calculating $n_{s\perp}(x,y)$ based on the parameters given in cases (a), (b), (c), (d), and (e) of Table I. In all figures the values of pairs density $n_{s\perp}$ have been normalized by $n_1=N/a_{\mathrm{op}}^2$.

polytropic index γ [defined by Eq. (3)] as a function of $1/(k_F^0 a_s)$. Note that the experimental result reported in Fig. 2 of Ref. [7] locates in the crossover regime $-1<1/(k_F^0 a_s)<1$, i.e., the three solid circles near $1/(k_F^0 a_s)=0$ in the inset.

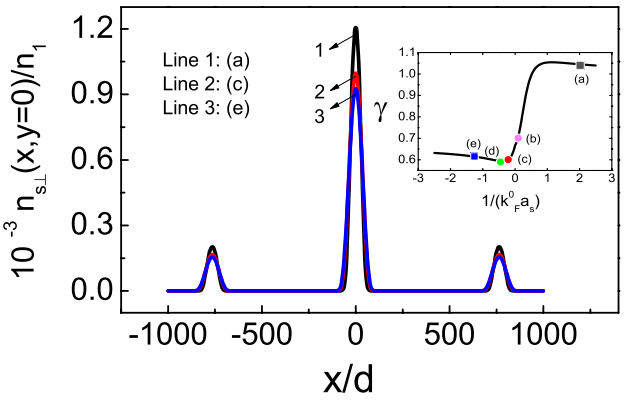

FIG. 3. (Color online) Number density distribution of condensed pairs $n_{s\perp}(x,y=0)$ in units of $n_1=N/a_{\rm op}^2$. The result is obtained by using the parameters of Table I for cases (a), (c), and (e). The inset is the polytropic index γ [defined by Eq. (3)] as a function of $1/(k_F^0 a_s)$. The experiment reported in Fig. 2 of Ref. [7] corresponds to the three solid circles near $1/(k_F^0 a_s)=0$ in the crossover regime.

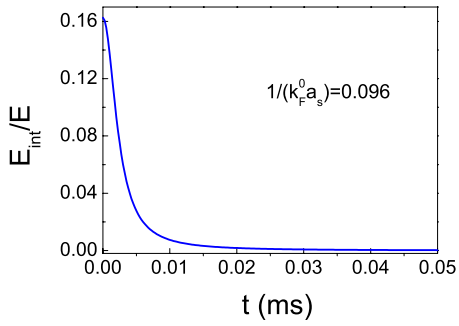

FIG. 4. (Color online) $E_{\rm int}(t)/E$ for $B=822$ G, i.e., $1/(k_F^0 a_s)=0.096$. t is the expansion time.

IV. DISCUSSION AND SUMMARY

In the calculations on the interference patterns presented in the preceding section, the interatoms interaction during the expansion has been neglected. It is necessary to make a simple estimation of the interaction during the expansion. The total energy of the system at time t reads

$$E(t)=E_{\rm kin}(t)+E_{\rm pot}(t)+E_{\rm int}(t), \tag{24}$$

where

$$E_{\rm kin}(t)=N\int_{-\infty}^{\infty}dx\int_{-\infty}^{\infty}dy\int_{-\infty}^{\infty}dz\frac{\hbar^2}{2M}|\nabla\Psi_s(\mathbf{r},t)|^2,$$

$$E_{\rm pot}(t)=N\int_{-\infty}^{\infty}dx\int_{-\infty}^{\infty}dy\int_{-\infty}^{\infty}dz[V_s^{\rm ho}(\mathbf{r})+V_s^{\rm op}(\mathbf{r})]|\Psi_s(\mathbf{r},t)|^2,$$

$$E_{\rm int}(t)=N\int_{-\infty}^{\infty}dx\int_{-\infty}^{\infty}dy\int_{-\infty}^{\infty}dz\frac{\mu_s(n_s)}{\gamma+1}|\Psi_s(\mathbf{r},t)|^2, \tag{25}$$

are the kinetic, potential, and interaction energies, respectively. Using the expression (16) it is easy to get $E_{\rm kin}(0)$, $E_{\rm pot}(0)$, and $E_{\rm int}(0)$. For example, for $B=822$ G [i.e., case (b) of Table I], we obtain $E_{\rm kin}(0)=E_{\rm pot}(0)=0.65\times10^{-23}$ J and $E_{\rm int}(0)=0.25\times10^{-23}$ J, and hence we have $E_{\rm int}(0)/E=0.16$, which means that in the ground state (i.e., before the expansion) the interatomic interaction takes an important role. To estimate the interaction energy during the expansion, we have calculated $E_{\rm int}(t)/E$ also for case (b) of Table I. The result is given in Fig. 4. We see that the interaction energy during the expansion can be neglected after 0.05 ms. Of course, during the expansion the weak interaction may induce some elastic collisions and hence a small change of the interference patterns of the subcondensates, a topic deserving further study. One can also consider possible Bragg diffraction and multiwave mixing in the superfluid Fermi gas in the BCS-BEC crossover by extending the work by Band *et al.* [38,39] for a weakly interacting Bose-Einstein condensed gas if some particular phase-matching conditions are assumed.

We must point out that the phenomenological approach on the interference patterns of ultracold Fermi gases presented here is valid only for zero temperature and for the superfluid state near BEC and the crossover regimes. (The results presented in Figs. 2–4 are for these regimes.) In the deep BCS regime (i.e., $\eta^0\ll-1$) and at any finite temperature, the BCS critical temperature drops quickly due to the fast decrease of atomic density during expansion and thus the superfluid cannot be maintained. In this case, our model cannot apply because the gas should expand according to a collisional hydrodynamics or enter a regime intermediate between collisional hydrodynamics and collisionless expansion [36].

In addition, in Ref. [7] the experimental results of the interference patterns from the superfluid regime to a Mott-insulator regime have also been reported by increasing the optical lattice depth sE_R. In a recent work, Zhai and Ho [40] studied the quantum phase transition between superfluid and band insulator of fermions in optical lattices. They showed that as one moves across Feshbach resonance to the BEC side, the superfluid-band insulator transition evolves into the superfluid-Mott-insulator transition. However, the experimental result on the change of the interference patterns from the superfluid regime to the Mott-insulator regime reported in Ref. [7] still remains to be explained.

In conclusion, based on a simple phenomenological approach we have investigated the interference patterns of a superfluid Fermi gas after releasing from both a harmonic oscillator and an optical lattice potential below and above Feshbach resonance. In order to obtain an initial distribution of the subcondensates formed in the optical lattice, we have solved the order-parameter equation [i.e., the GNLS Eq. (5)] which is valid for the crossover from Bardeen-Cooper-Schrieffer superfluid to a Bose-Einstein condensate. Then we have discussed the coherent dynamic evolution of the subcondensates during a nearly ballistic expansion after the harmonic oscillator and optical lattice potentials are switched off. The interference patterns of the superfluid Fermi gas along the BCS-BEC crossover during the expansion have been calculated by using the Feynman propagator method combined with numerical simulations. The results obtained for interference patterns for superfluid Fermi gases in a BCS-BEC crossover agree fairly well with the recent experimental ones reported in Ref. [7].

ACKNOWLEDGMENTS

This work was supported by NSF-China under Grants No. 90403008 and No. 10674060, by the Key Development Program for Basic Research of China under Grants No. 2005CB724508 and No. 2006CB921104, and by the Program for Changjiang Scholars and Innovative Research Team of Chinese Ministry of Education.

[1] Q. Chen *et al.*, Phys. Rep. **412**, 1 (2005).
[2] I. Bloch *et al.*, e-print arXiv:0704.3011v1.
[3] S. Giorgini *et al.*, e-print arXiv:0706.3360v1, and reference therein.
[4] C. J. Pethick and H. Smith, *Bose-Einstein Condensation in Dilute Gases* (Cambridge University Press, Cambridge, UK, 2002).
[5] L. Pitaevskii and S. Stringari, *Bose-Einstein Condensates* (Clarendon Press, Oxford, 2003).
[6] O. Morsch and M. Oberthaler, Rev. Mod. Phys. **78**, 179 (2006).
[7] J. K. Chin *et al.*, Nature (London) **443**, 961 (2006).
[8] G. S. Nunes, J. Phys. B **32**, 4293 (1999).
[9] Y. E. Kim and A. L. Zubarev, Phys. Rev. A **70**, 033612 (2004); J. Catani, L. De Sarlo, G. Barontini, F. Minardi, and M. Inguscio, *ibid.* **77**, 011603(R) (2008).
[10] N. Manini and L. Salasnich, Phys. Rev. A **71**, 033625 (2005).
[11] T. K. Ghosh and K. Machida, Phys. Rev. A **73**, 013613 (2006).
[12] G. Diana, N. Manini, and L. Salasnich, Phys. Rev. A **73**, 065601 (2006).
[13] J. Yin, Y. L. Ma, and G. Huang, Phys. Rev. A **74**, 013609 (2006).
[14] L. Salasnich and N. Manini, Laser Phys. **17**, 169 (2007).
[15] Y. Zhou and G. Huang, Phys. Rev. A **75**, 023611 (2007).
[16] W. Wen and G. Huang, Phys. Lett. A **362**, 331 (2007).
[17] Y.-L. Ma and G. Huang, Phys. Rev. A **75**, 063629 (2007).
[18] G. E. Astrakharchik, J. Boronat, J. Casulleras, and S. Giorgini, Phys. Rev. Lett. **93**, 200404 (2004).
[19] J. Carlson, S. Y. Chang, V. R. Pandharipande, and K. E. Schmidt, Phys. Rev. Lett. **91**, 050401 (2003); S.-Y. Chang, V. R. Pandharipande, J. Carlson, and K. E. Schmidt, Phys. Rev. A **70**, 043602 (2004).
[20] An interpolating analytical formula for $\varepsilon(n)$ has been given in Ref. [10] for ^{6}Li.
[21] C. Menotti, P. Pedri, and S. Stringari, Phys. Rev. Lett. **89**, 250402 (2002).
[22] H. Heiselberg, Phys. Rev. Lett. **93**, 040402 (2004).
[23] H. Hu, A. Minguzzi, X. J. Liu, and M. P. Tosi, Phys. Rev. Lett. **93**, 190403 (2004).
[24] P. Pieri and G. C. Strinati, Phys. Rev. Lett. **91**, 030401 (2003).
[25] P. Pedri, L. Pitaevskii, S. Stringari, C. Fort, S. Burger, F. S. Cataliotti, P. Maddaloni, F. Minardi, and M. Inguscio, Phys. Rev. Lett. **87**, 220401 (2001).
[26] X. Zhi-Jun, C. Cheng, and X. Hong-Wei, Chin. Phys. Lett. **20**, 611 (2003); S. Liu *et al.*, J. Phys. B **36**, 2083 (2003).
[27] R. P. Feynman and A. R. Hibbs, *Quantum Mechanics and Path Integrals* (McGraw-Hill, New York, 1965).
[28] J. Tempere and J. T. Devreese, Solid State Commun. **113**, 471 (2000).
[29] M. R. Andrews *et al.*, Science **275**, 637 (1997).
[30] B. P. Anderson and M. A. Kasevich, Science **282**, 1686 (1998).
[31] M. Greiner *et al.*, Nature (London) **415**, 39 (2002).
[32] T. Bourdel, J. Cabizolles, L. Khaykovich, K. M. F. Magalhaes, S. J. J. M. F. Kokkelsmans, G. V. Shlyapnikov, and C. Salomon, Phys. Rev. Lett. **91**, 020402 (2003).
[33] C. A. Regal, M. Greiner, and D. S. Jin, Phys. Rev. Lett. **92**, 040403 (2004); M. W. Zwierlein, C. A. Stan, C. H. Schunck, S. M. F. Raupach, A. J. Kerman, and W. Ketterle, *ibid.* **92**, 120403 (2004).
[34] M. W. Zwierlein *et al.*, Nature (London) **435**, 1047 (2005).
[35] C. A. Regal, M. Greiner, S. Giorgini, M. Holland, and D. S. Jin, Phys. Rev. Lett. **95**, 250404 (2005).
[36] C. H. Schunck, M. W. Zweirlein, A. Schirotzek, and W. Ketterle, Phys. Rev. Lett. **98**, 050404 (2007).
[37] The theoretical modeling of the fast magnetic field ramp is not an easy problem which needs an investigation of the implementation of a time-dependent description of the scattering length. For detail, see Sec. XI of Ref. [3].
[38] Y. B. Band, M. Trippenbach, J. P. Burke, and P. S. Julienne, Phys. Rev. Lett. **84**, 5462 (2000).
[39] M. Trippenbach, Y. B. Band, and P. S. Julienne, Phys. Rev. A **62**, 023608 (2000).
[40] H. Zhai and T.-L. Ho, Phys. Rev. Lett. **99**, 100402 (2007).